Jelena M. Djoković
Professor
University of Belgrade
Technical faculty of Bor
Bor, Serbia

Ružica R. Nikolić
Faculty of Civil Engineering
University of Žilina
Žilina, Slovakia

Josef Vičan
Faculty of Civil Engineering
University of Žilina
Žilina, Slovakia

Dalibor Djenadić
Assistant
University of Belgrade
Technical faculty of Bor
Bor, Serbia

Dynamic Growth of an Interfacial Crack Between the Two Anisotropic Materials

In this paper is considered behavior of the stress field around the tip of a crack that propagates dynamically along the interface between the two anisotropic materials. The emphasis is set on application and extension of the existing concept of the interfacial fracture mechanics to problem of a crack that propagates dynamically. The angular distribution of the stress is presented. The behavior of the oscillatory index, force resolution factor and energy factor in terms of the crack tip speed and ratio of materials' stiffnesses was studied. The oscillatory index value increases with increase of the crack propagating speed and it tends to infinity when the speed approaches the Rayleigh wave speed of the softer of the two materials. The force resolution factor strongly depends on the crack tip speed, but weakly on the stiffnesses ratio. The opposite is valid for the energy factor. In this work, the dynamic stress intensity factor was determined of the anisotropic bimaterial combination for several basic configurations. Result obtained in this paper can serve as a guide in materials mathematical modeling..

Keywords: *Interface, crack, dynamic growth, anisotropy.*

1. INTRODUCTION

Scientific explanation of the initiation and growth mechanisms of a crack on a bimaterial interface is fundamental for understanding the fracture process in materials like composites and ceramics. The very important mechanism of fracture of fiber-reinforced composites and whisker-reinforced ceramics is, for instance, debonding between the substrate and reinforcing phases. This failure process can be quasi-static or dynamic, depending on the type of loading to which the composite structure is subjected.

Due to complexity of the problem, there are only a few theoretical results of dynamic crack growth of some fracture problems. Those results provided insight in the dynamic behavior only in the immediate vicinity of the crack tip. In order to formulate a mechanism of initiation and dynamic crack growth at bimaterial interfaces, it is necessary to know the complete spatial structure of the stress and strain fields that surround the tip of a moving interfacial crack.

Experimental investigations of deformation fields at the tip of the interfacial crack were carried out by Tippur and Rosakis (1991) and Rosakis et al. (1991) using an optical method of the Coherent Gradient Sensor (CGS) and very high-speed photography. The bimaterial system that they used was the PMMA (polymethylmetacylate)/Aluminum combination. The considered speeds were up to 90 % of Rayleigh's wave speed for PMMA. Guided by this investigation, Yang et al. (1991) obtained structure of the elastodynamic field in steady state growth conditions of an interfacial crack. Furthermore, Deng (1992) gave the asymptotic series representation of the stress field near the tip of a running interfacial crack in a bimaterial system under steady-state conditions. Also, inspired by experiments of Tippur and Rosakis's (1991), Lo et al. (1992) have performed a numerical analysis of the same bimaterial system as was used in the experiments. In paper of Liu, Lambros and Rosakis (1993) is given the asymptotic structure of the near tip fields for a crack in bimaterial system, for the non-uniform crack growth. Using the programming package *Mathematica*®, Nikolic and Djokovic (2009), analyzed the structure of the strain field in terms of the non-uniform growth of crack on bimaterial interface. All of those analyses were related to the elastic isotropic body.

For anisotropic bodies, the non-uniform crack growth in terms of Mode I is investigated by Willis (1992), while Nikolic et al. (2010), analyzed the structure of the stress field at the crack tip that dynamically propagates along the interface between two orthotropic materials.

2. PROBLEM FORMULATION

For the dynamic crack propagation case, shown in Figure 1, the equilibrium equations are substituted by the equations of motion, which are, in the absence of the volume forces, given as:

$$C_{ijkl}\frac{\partial^2 u_k}{\partial x_l \partial x_i} = \rho \ddot{u}_j \tag{1}$$

The stiffness tensor C_{ijkl} and the material density ρ have different values for materials 1 and 2. Superscripts $^{(1)}$ and $^{(2)}$ will be attached when distinction is necessary. It is assumed that material 1 has the lower value of the Rayleigh's wave speed c_R, as well as that the crack propagates with the velocity $v = \dot{\ell}(t)$, which is smaller than c_R.

Received: May 2014, Accepted: June 2014
Correspondence to: Jelena Djokovic
Technical faculty of Bor,
Vojske Jugoslavije 12, 19210 Bor, Serbia
E-mail: jelenamdjokovic@gmail.com
doi:10.5937/fmet1403229D

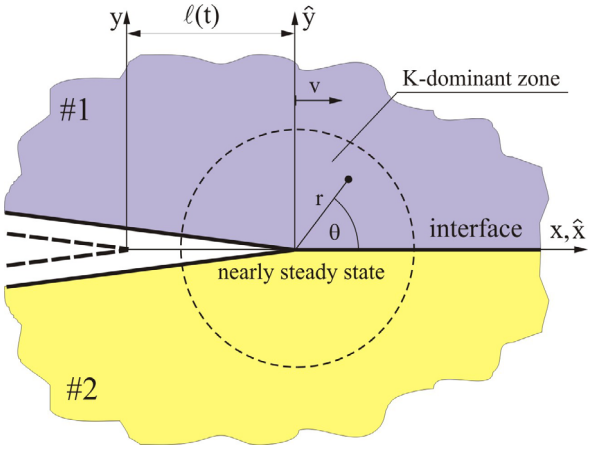

Figure 1. Schematic representation of the dynamic crack growth along a bimaterial interface

The movable coordinate system $(\hat{x}, \hat{y})$ is fixed at the crack tip. Thus, for the movable system, equations (1) become:

$$C_{\alpha jk\beta}u_{k,\alpha\beta} = 0\,,\ \alpha,\beta = 1,2 \tag{2}$$

where $(\ )_{,\alpha} = \partial(\ )/\partial\hat{x}_\alpha$. Elastic constants depend on the crack tip velocity v, in the following way:

$$\hat{C}_{\alpha jk\beta} = C_{\alpha jk\beta} - \rho v^2 \delta_{jk}\delta_{1\alpha}\delta_{1\beta} \tag{3}$$

where δ_{ij} is Kronecker's delta and $\hat{C}_{\beta jk\alpha} = \hat{C}_{\alpha jk\beta}$.

For the orthotropic materials, for the planar problem, elastic constants are:

$$\begin{pmatrix} C_{11} & C_{12} & 0 \\ C_{12} & C_{22} & 0 \\ 0 & 0 & C_{66} \end{pmatrix}. \tag{4}$$

The following variables: $\lambda_1 = \dfrac{(C_{11}/C_{66})\alpha_1^2 + p_1^2}{(C_{12}/C_{66}+1)p_1}$, $\lambda_2 = \dfrac{(C_{22}/C_{66})\alpha_1^2 + p_2^2}{(C_{12}/C_{66}+1)p_2}$ are introduced, where p_1 and p_2 represent the solutions with the positive imaginary parts, of the characteristic equation of the fourth order:

$$p^4 + 2s\xi p^2 + \xi^2 = 0 \tag{5}$$

where

$$\xi = \alpha_1\alpha_2\sqrt{\frac{C_{11}}{C_{22}}}\,,$$

$$s = \frac{\alpha_2^2 + (C_{11}C_{22}/C_{66}^2)\alpha_1^2 - (1 + C_{12}/C_{66})^2}{2\sqrt{(C_{11}C_{22}/C_{66}^2)\alpha_1\alpha_2}} \tag{6}$$

and

$$\alpha_1 = \sqrt{1 - \frac{\rho v^2}{C_{11}}}\,,\quad \alpha_2 = \sqrt{1 - \frac{\rho v^2}{C_{66}}}\,. \tag{7}$$

The roots p_1 and p_2 of the equation (5), are:

$$p_1,\ p_2 = \begin{cases} \mathrm{i}\sqrt{\xi\left[\sqrt{(s+1)/2} \pm \sqrt{(s-1)/2}\right]} & \text{if } s \geq 1 \\ \sqrt{\xi\left[\pm\sqrt{(1-s)/2} + \mathrm{i}\sqrt{(1+s)/2}\right]} & \text{if } -1 < s < 1 \end{cases}$$

Two Hermitian matrices necessary to the analysis, **B** and **H** are defined by:

$$\mathbf{B} = \mathrm{i}\mathbf{A}\mathbf{L}^{-1}\,,\quad \mathbf{H} = \mathbf{B}^{(1)} + \overline{\mathbf{B}}^{(2)}\,. \tag{9}$$

The matrices from equation (9) are defined in Nikolic at al. (2010) and for case of two orthotropic materials become:

$$\mathbf{A} = \begin{bmatrix} 1 & -\dfrac{1}{\lambda_2} \\ -\lambda_1 & 1 \end{bmatrix}$$

$$\mathbf{L} = C_{66}\begin{bmatrix} p_1 - \lambda_1 & 1 - \dfrac{p_2}{\lambda_2} \\ \dfrac{C_{12}}{C_{66}} - \dfrac{C_{22}}{C_{66}}p_1\lambda_1 & -\dfrac{C_{12}}{C_{66}\lambda_2} + \dfrac{C_{22}}{C_{66}}p_{21} \end{bmatrix} \tag{10}$$

and

$$\mathbf{B} = \frac{1}{C_{66}R}\begin{bmatrix} \dfrac{C_{22}}{C_{66}}\alpha_2^2\sqrt{\dfrac{2(1+s)}{\xi}} & \mathrm{i}\left(\dfrac{C_{22}}{C_{66}} - \dfrac{\alpha_2^2\,C_{12}/C_{66}}{\xi}\right) \\ -\mathrm{i}\left(\dfrac{C_{22}}{C_{66}} - \dfrac{\alpha_2^2\,C_{12}/C_{66}}{\xi}\right) & \dfrac{C_{22}}{C_{66}}\sqrt{2\xi(1+s)} \end{bmatrix} \tag{11}$$

where R is the Rayleigh's wave function, defined as:

$$R = \frac{C_{22}}{C_{66}}\left(\frac{C_{22}}{C_{66}}\xi - 1 + \alpha_2^2\right) - \left(\frac{C_{12}}{C_{66}}\right)^2\frac{\alpha_2^2}{\xi}\,. \tag{12}$$

Rayleigh's wave speed c_R is a solution of equation (11) for R=0. The matrix **H**, according to Nikolic at al. (2010), for the two orthotropic materials is defined by:

$$\mathbf{H} = \begin{pmatrix} H_{11} & iH_{12} \\ -iH_{12} & H_{22} \end{pmatrix}. \tag{13}$$

3. CRACK TIP STRESS FIELD

For analyzing the problem of a crack on the interface between the two anisotropic materials, the 3×3 matrix **H** is used, which depends on elastic constants of both materials and which has the modulus of elasticity dimensions. The structure of the stress field at the crack tip which propagates dynamically is described by equation, Yang et al. (1991):

$$\overline{\mathbf{H}}\mathbf{w} = e^{2\pi\varepsilon}\mathbf{H}\mathbf{w} \tag{14}$$

where: **w** is the unit vector, $e^{2\pi\varepsilon}$ is the Eigen value. The three obvious Eigen values pairs are: $(\varepsilon, \mathbf{w})$, $(-\varepsilon, \overline{\mathbf{w}})$ and $(0, \mathbf{w}_3)$. The oscillation index ε is given by, Rice (1988):

$$\varepsilon = \frac{1}{2\pi}\ln\frac{1-\beta}{1+\beta} \tag{15}$$

where β is one of the two Dundurs's parameters that is defined by:

$$\beta = -\sqrt{-\frac{1}{2}tr\left\{\left(\frac{\mathrm{Im}\,\mathbf{H}}{\mathrm{Re}\,\mathbf{H}}\right)^2\right\}}\,. \tag{16}$$

where tr{} denotes the matrix trace. The Eigen vectors **w** and $\mathbf{w}_3$ are the complex and real variable, respectively, and all of these variables are dimensionless

The near tip stress field for an interface crack is a linear combination of the two types of fields, a coupled oscillatory field, defined by a complex stress intensity factor *K*, and a non-oscillatory field, scaled by a real stress intensity factor K_3, Hutchinson and Suo (1992):

$$\sigma_{ij} = \frac{1}{\sqrt{2\pi r}}\left[\mathrm{Re}(Kr^{i\varepsilon})\tilde{\sigma}_{ij}^{1}(\theta,\varepsilon) + \mathrm{Im}(Kr^{i\varepsilon})\tilde{\sigma}_{ij}^{2}(\theta,\varepsilon) + K_3\tilde{\sigma}_{ij}^{3}(\theta)\right] \tag{17}$$

where r and θ are polar coordinates and *i*, *j* = *x*, *y*, *z*, $\tilde{\sigma}_{ij}^{1,2,3}(\theta)$ are the angular functions which correspond to tensile tractions, in-plane shear tractions and anti-plane shear tractions across the interface, respectively, and are defined in the Appendix. The two stress intensity factors have different dimensions: K= [stress] [length] $^{1/2-i\varepsilon}$ and K_3= [stress] [length] $^{1/2}$. The interfacial force, which has the components $\mathbf{t}=\{\sigma_{yi}\}=\{\sigma_{yx}, \sigma_{yy}, \sigma_{yz}\}$, can be written by use of the Eigen vectors as:

$$\mathbf{t} = t\mathbf{w} + \bar{t}\bar{\mathbf{w}} + t_3\mathbf{w}_3\,, \tag{18}$$

where: t, $\bar{t}$ i t_3 are the force vector components, and $t = t_2 + it_1$ are the complex and t_3 real variables, respectively. In the general case, the following hold $t \neq \sigma_{yy} + i\sigma_{yx}$ and $t_3 \neq \sigma_{yz}$. When r→0, the force components on the interface, ahead of the crack tip, are:

$$t(r) = \frac{Kr^{i\varepsilon}}{\sqrt{2\pi r}}\,,\ t_3(r) = \frac{K_3}{\sqrt{2\pi r}}\,. \tag{19}$$

Considering that $r^{i\varepsilon} = e^{i\varepsilon\ln r} = \cos(\varepsilon\ln r) + i\sin(\varepsilon\ln r)$, the force component $t = t_2 + it_1$ rotates with variation of *r*. The physical meaning of the unit vectors **w** and $\mathbf{w}_3$ is obvious: the projection of the $\mathbf{t}_3$ component onto $\mathbf{w}_3$ has the square root properties. In the plane whose axes are Re(**w**) and Im(**w**) the component t rotates and has the square root characteristics.

The crack opening displacement vector is:

$$\boldsymbol{\delta}(r) = (\mathbf{H}+\bar{\mathbf{H}})\sqrt{\frac{r}{2\pi}}\left[\frac{Kr^{i\varepsilon}\mathbf{w}}{(1+2i\varepsilon)\cosh\pi\varepsilon} + \frac{\bar{K}r^{-i\varepsilon}\bar{\mathbf{w}}}{(1-2i\varepsilon)\cosh\pi\varepsilon} + K_3\mathbf{w}_3\right] \tag{20}$$

The relation between the two energy release rates *K* and K_3 and the energy release rate is:

$$G = \frac{\bar{\mathbf{w}}^T(\mathbf{H}+\bar{\mathbf{H}})\mathbf{w}}{4\cosh^2\pi\varepsilon}|K|^2 + \frac{1}{8}\mathbf{w}_3^T(\mathbf{H}+\bar{\mathbf{H}})\mathbf{w}_3K_3^2 \tag{21}$$

For the case of the two orthotropic materials, with the two mutually perpendicular axes and interface in the direction of the *x*-axis, the matrix **H** components are, Wang et al. (1992):

$$\begin{aligned}
H_{11} &= \left[2n\sqrt[4]{\lambda}\sqrt{s_{11}s_{22}}\right]_1 + \left[2n\sqrt[4]{\lambda}\sqrt{s_{11}s_{22}}\right]_2\\
H_{22} &= \left[2n\frac{1}{\sqrt[4]{\lambda}}\sqrt{s_{11}s_{22}}\right]_1 + \left[2n\frac{1}{\sqrt[4]{\lambda}}\sqrt{s_{11}s_{22}}\right]_2\\
H_{12} &= \bar{H}_{21} = i\left[\sqrt{s_{11}s_{22}} + s_{12}\right]_1 - \left[\sqrt{s_{11}s_{22}} + s_{12}\right]_2\\
H_{33} &= \left[\sqrt{s_{44}s_{55}}\right]_1 + \left[\sqrt{s_{44}s_{55}}\right]_2\\
H_{13} &= H_{23} = H_{31} = H_{32} = 0
\end{aligned} \tag{22}$$

where $[\,]_1$ denotes values for material 1, and $[\,]_2$ denotes values for material 2, and:

$$s_{11} = \frac{1}{E_1},\ s_{22} = \frac{1}{E_2},\ s_{66} = \frac{1}{G_{12}},\ s_{12} = -\frac{\nu_{12}}{E_1} = -\frac{\nu_{21}}{E_2},$$

$$\lambda = \frac{s_{11}}{s_{22}} = \frac{E_2}{E_1},\ n = \sqrt{\frac{(1+\rho)}{2}},$$

$$\rho = \frac{2s_{12}+s_{66}}{2\sqrt{s_{11}s_{22}}} = \frac{\sqrt{E_1E_2}}{2G_{12}} - \sqrt{\nu_{12}\nu_{21}}\,.$$

Parameters λ and ρ measure anisotropy in the sense that for λ = 1 material has the cubic symmetry and for $\lambda = \rho = 1$ material is isotropic.

Dundurs parameter β for the case of orthotropic material is defined by:

$$\beta = \frac{iH_{12}}{\sqrt{H_{11}H_{22}}} \tag{23}$$

the Eigenvectors have the form:

$$w = \left\{-\frac{i}{2}\sqrt{\frac{H_{22}}{H_{11}}},\ \frac{1}{2},\ 0\right\},\quad w_3 = \{0,\ 0,\ 1\} \tag{24}$$

The force components on the interface, are:

$$t = \sigma_{yy} + i\sqrt{\frac{H_{11}}{H_{22}}}\sigma_{xy}\,,\qquad t_3 = \sigma_{zy} \tag{25}$$

The complex component, as can be seen from equation (25), has the multiplier, Nikolic and Djokovic (2011):

$$\eta = \sqrt{\frac{H_{11}}{H_{22}}}\,, \tag{26}$$

which for the majority of polymers ranges between 1 and 2, and which is called the traction resolution factor, Djokovic i Nikolic (2012).

The relation between the energy release rate and *K* and K_3 is:

$$G = \frac{\tau}{4C_{66}^{(1)}}|K|^2 + \frac{1}{4}H_{33}K_3^2\,, \tag{27}$$

where τ is the dimensionless real parameter which is called the energy factor and it has the form, Djokovic i Nikolic (2012):

$$\tau = C_{66}^{(1)}(H_{22} - \frac{H_{12}^2}{H_{11}}). \quad (28)$$

Parameters ε, η and τ depend on the speed of the crack tip. In Figure 2 is shown the dependence of parameters ε, η and τ on the speed of the crack tip for material combination with identical densities and Poisson's ratio of 0.3.

From the Figure 2(a) one can see that, the oscillatory index, ε, increases with crack tip speed, v. In Figure 2(a) is shown the variation of the oscillatory index as a function of the stiffnesses ratio $\lambda = C_{66}^{(2)} / C_{66}^{(1)}$, where this ratio ranges from 1, for the case of the isotropic material, to 10, for the case of the large difference in stiffnesses. The oscillatory index increases with the increase of the difference in stiffnesses. It can be seen that for $v \approx 0.8\, c_R$ the dynamic oscillatory index is twice bigger than for the stationary case value.

Figure 2(b) shows that the traction resolution factor, η, weakly depends on the stiffnesses ratio but strongly depends on the speed of the crack tip. This means that the mode mixity changes with speed of the crack. This is significantly different from the behavior of the energy factor, τ, as seen from Figure 2(c).

In Figures 3 and 4 are shown the Mode I and Mode II angular stresses distribution for three different values of crack tip speed and two stiffness ratio, λ = 1 and λ = 10.

From Figure 3 one can see that, the maximum of the hoop stress, $\sigma_{\theta\theta}$, under Mode I loading at high crack tip speed is at about 60° from the crack plane for the isotropic material (λ=1), what suggests that the dynamic branching of a crack has to be taken into account. For anisotropic material, for the case of the large difference in stiffnesses (λ=10), value of this stress is even higher, which means that the interfacial crack may have branch out, in terms of dynamic crack growth. Figure 3 shows also that, at high crack tip speed, in material below the interface, material 2, develops a significant radial stress, σ_{rr},. This could be cause cracks on the substrate as the main crack propagates. Figure 4 shows that the effect of differences in the materials through an interface on the angular stress distribution is less pronounced under the Mode II loading.

Dynamic stress intensity factors for a semi-infinite crack on an interface between two anisotropic materials are, Yang et al. (1991):

$$K^d = -\sqrt{\frac{2}{\pi}} \cosh \pi\varepsilon \int_{-\infty}^{0} (-\hat{x})^{-\frac{1}{2}-i\varepsilon} t(\hat{x}) d\hat{x}$$
$$K_3^d = -\sqrt{\frac{2}{\pi}} \int_{-\infty}^{0} (-\hat{x})^{-\frac{1}{2}} t_3(\hat{x}) d\hat{x}\,, \quad (29)$$

where t and t_3 are defined in equation (25). Dynamic stress intensity factors for a central crack of length $2a$ subjected to remote uniform stresses on an interface between two anisotropic materials are, Yang et al. (1991):

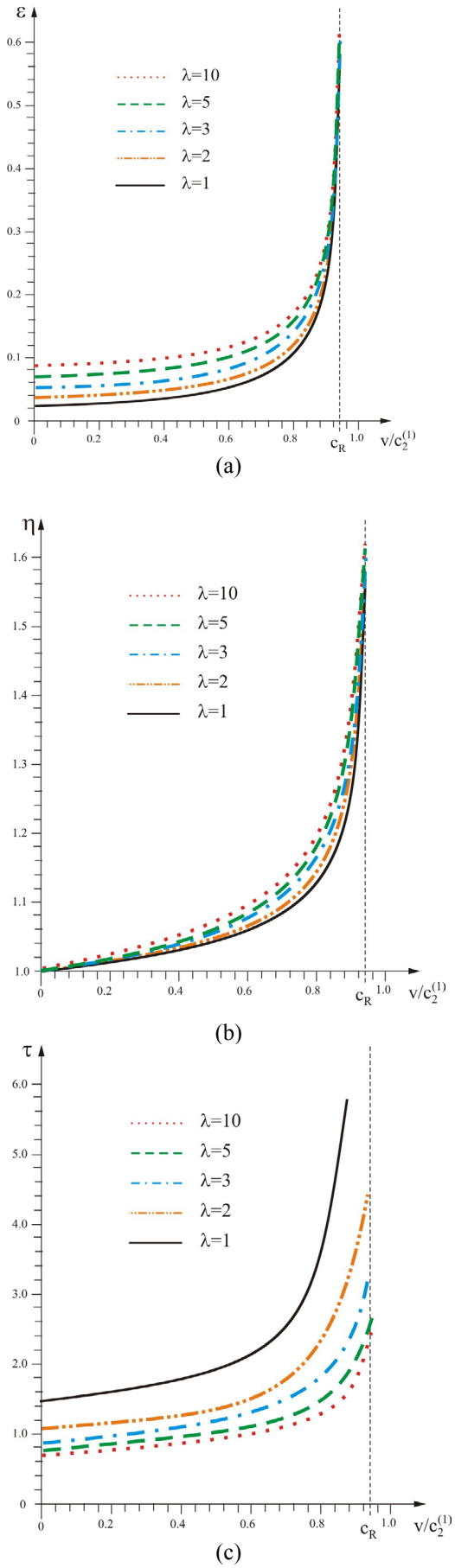

Figure. 2. Dependence of: (a) the oscillatory index, ε, (b) the traction resolution factor, η and (c) the energy factor, τ, on the crack propagation velocity.

$$K^d = -\sqrt{\frac{2}{\pi}}\cosh \pi\varepsilon (2a)^{-\frac{1}{2}-i\varepsilon} \int_{-a}^{a} \left(\frac{a+\hat{x}}{a-\hat{x}}\right)^{\frac{1}{2}+i\varepsilon} t(\hat{x})d\hat{x}$$
$$K_3^d = -\sqrt{\frac{1}{\pi a}} \int_{-a}^{a} \left(\frac{a+\hat{x}}{a-\hat{x}}\right)^{\frac{1}{2}} t_3(\hat{x})d\hat{x} \,. \tag{30}$$

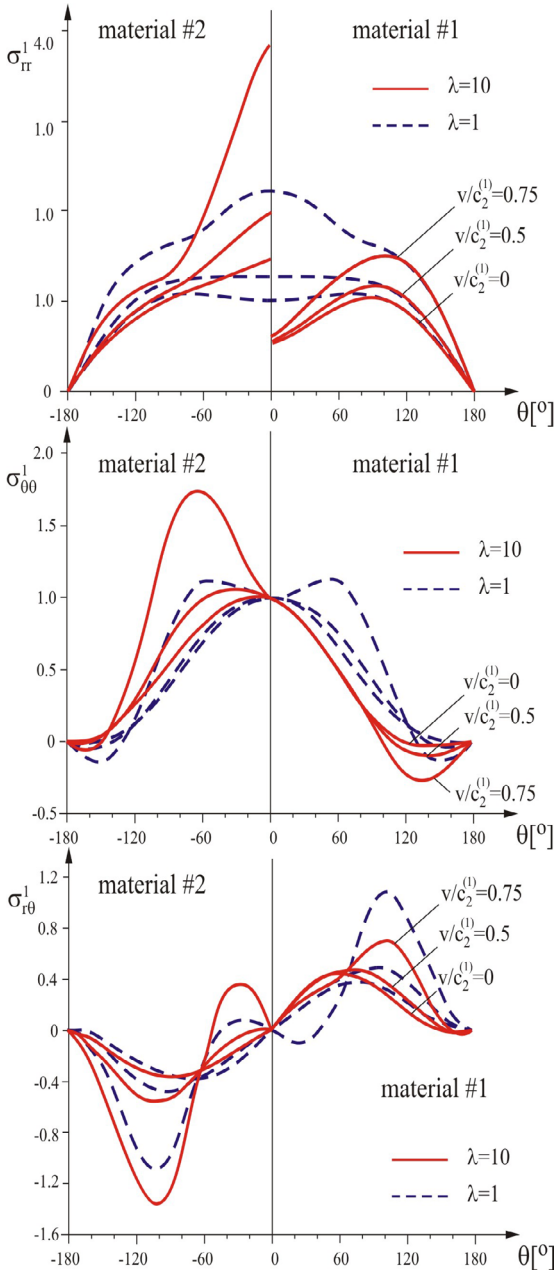

Figure 3. Angular variation of stresses for a bimaterial combination for different values of crack tip speed under the Mode I loading

In general case, for the crack that propagates dynamically in the homogeneous isotropic material, dynamic stress intensity factor, for the current crack of the length l and crack speed v can be written as, Freund (1990):

$$K_I^d(l,\upsilon) = k_I(\upsilon)K_I(l,0)\,, \tag{31}$$

where $K_I(l, 0)$ is the static stress intensity factor for Mode I, while $k_I(\upsilon)$ is the universal dimensionless function which depends on crack speed and elastic constants. This factorization is valid for the other two Modes of crack growth, as well.

Analogously to equation (31), for the crack that propagates dynamically along the interface, a relationship can be established between the stress intensity factor for the stationary crack $K(l, 0)$ and dynamic complex stress intensity factor $K^d(l, \upsilon)$. It is assumed that the crack extension υt is small with respect to other relevant dimensions and that this is the only length in the problem. Based on linearity of the problem and dimensional analysis, one can write:

$$K^d(l,\upsilon) = (\upsilon t)^{-i\varepsilon}[(\upsilon t)^{i\varepsilon_0} k_1(\upsilon)K(l,0) + \\ + (\upsilon t)^{-i\varepsilon_0} k_2(\upsilon)\bar{K}(l,0)]\,, \tag{32}$$

where ε_0 is the static oscillatory index, ε is the oscillatory index for speed υ and $k_1(\upsilon)$ and $k_2(\upsilon)$ are the universal dimensionless functions that depend on crack speed and elastic constants.

4. CONCLUSION

In this paper is considered the behavior of the characteristic parameters of dynamic crack propagation along the interface between two anisotropic materials. The emphasis is on the application of the fracture mechanics concept for the interfacial crack that propagates dynamically, at high speed. In this work is analyzed the behavior of three characteristic parameters of dynamic fracture, namely: the oscillatory index, the traction resolution factor and the energy factor depending on the speed of the crack tip and stiffnesses ratio.

It was noted that the value of the oscillatory index increases with the speed of crack propagation and tends to infinity as velocity approaches the Rayleigh wave speed of the less stiffer of the two materials. The traction resolution factor strongly depends on the speed of the crack tip, but weakly on the stiffness ratio. This means that the mode mixity changes with speed. The energy factor acts contrary to the traction resolution factor, with increasing speed of the crack tip, i.e. it depends more on the stiffnesses ratio than the speed of the crack tip.

The angular stress distribution ahead of the crack tip along the interface between the two anisotropic materials for different values of crack tip speed are shown in this paper. Based on that, it can be concluded that dynamic crack growth along the interface between two anisotropic materials is followed by a series of events that are not encountered in homogeneous materials or in the case of steady state conditions of growth of the interfacial crack between isotropic materials.

In this paper are also given expressions for dymanic stress intensity faktors for anisotropic bimaterials for the two basic configurations on an interface, a semi-infinite crack and a central crack.

Results presented in this paper can serve as guidelines for micromechanical modeling of materials, because, for composite materials, analysis of dynamic crack propagation along the interface will help to model and to design against failure.

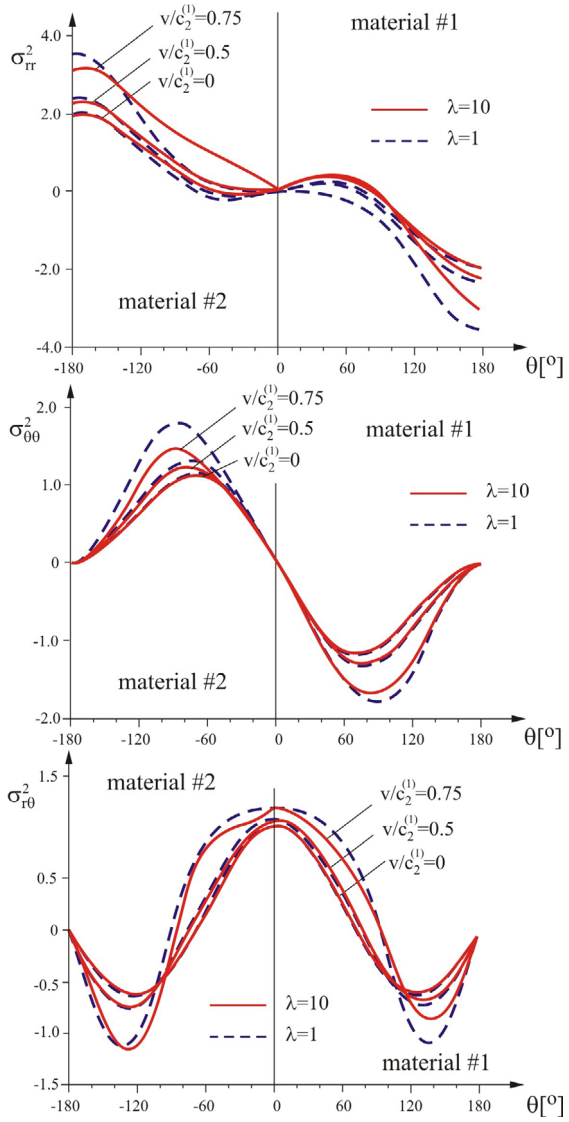

Figure 4. Angular variation of stresses for a bimaterial combination for different values of crack tip speed under the Mode II loading

APPENDIX

Angular functions in equation (17) for $0 \le \theta \le \pi$, have the form:

$$\tilde{\sigma}_{11}^{1}(\theta,\varepsilon)=\frac{1}{D\cosh\pi\varepsilon}\left\{\begin{array}{l}\frac{(1+2\alpha_1^2-\alpha_2^2)}{\sqrt{\gamma_1}}(P_{11}\cos\varepsilon_1\cos\frac{\theta_1}{2}+\\+P_{12}\sin\varepsilon_1\sin\frac{\theta_1}{2})+\\+\frac{2\alpha_2}{\sqrt{\gamma_2}}(P_{21}\cos\varepsilon_2\cos\frac{\theta_2}{2}+\\+P_{22}\sin\varepsilon_2\sin\frac{\theta_2}{2})\end{array}\right.$$

$$\tilde{\sigma}_{12}^{1}(\theta,\varepsilon)=\frac{1}{D\cosh\pi\varepsilon}\left\{\begin{array}{l}\frac{-2\alpha_1}{\sqrt{\gamma_1}}(P_{12}\sin\varepsilon_1\cos\frac{\theta_1}{2}-\\-P_{11}\cos\varepsilon_1\sin\frac{\theta_1}{2})+\\+\frac{(1+\alpha_2^2)}{\sqrt{\gamma_2}}(P_{21}\cos\varepsilon_2\sin\frac{\theta_2}{2}-\\-P_{22}\sin\varepsilon_2\cos\frac{\theta_2}{2})\end{array}\right.$$

$$\tilde{\sigma}_{22}^{1}(\theta,\varepsilon)=\frac{1}{D\cosh\pi\varepsilon}\left\{\begin{array}{l}\frac{-(1+\alpha_2^2)}{\sqrt{\gamma_1}}(P_{11}\cos\varepsilon_1\cos\frac{\theta_1}{2}+\\+P_{12}\sin\varepsilon_1\sin\frac{\theta_1}{2})+\\+\frac{2\alpha_2}{\sqrt{\gamma_2}}(P_{21}\cos\varepsilon_2\cos\frac{\theta_2}{2}+\\+P_{22}\sin\varepsilon_2\sin\frac{\theta_2}{2})\end{array}\right.$$

$$\tilde{\sigma}_{11}^{2}(\theta,\varepsilon)=\frac{1}{D\cosh\pi\varepsilon}\left\{\begin{array}{l}\frac{(1+2\alpha_1^2-\alpha_2^2)}{\sqrt{\gamma_1}}(P_{12}\cos\varepsilon_1\sin\frac{\theta_1}{2}-\\-P_{11}\sin\varepsilon_1\cos\frac{\theta_1}{2})+\\+\frac{2\alpha_2}{\sqrt{\gamma_2}}(P_{22}\cos\varepsilon_2\sin\frac{\theta_2}{2}-\\-P_{21}\sin\varepsilon_2\cos\frac{\theta_2}{2})\end{array}\right.$$

$$\tilde{\sigma}_{12}^{2}(\theta,\varepsilon)=\frac{1}{D\cosh\pi\varepsilon}\left\{\begin{array}{l}\frac{-2\alpha_1}{\sqrt{\gamma_1}}(P_{12}\cos\varepsilon_1\cos\frac{\theta_1}{2}+\\+P_{11}\sin\varepsilon_1\sin\frac{\theta_1}{2})-\\-\frac{(1+\alpha_2^2)}{\sqrt{\gamma_2}}(P_{22}\cos\varepsilon_2\cos\frac{\theta_2}{2}+\\+P_{21}\sin\varepsilon_2\sin\frac{\theta_2}{2})\end{array}\right.$$

$$\tilde{\sigma}_{22}^{2}(\theta,\varepsilon)=\frac{1}{D\cosh\pi\varepsilon}\left\{\begin{array}{l}\frac{-(1+\alpha_2^2)}{\sqrt{\gamma_1}}(P_{12}\cos\varepsilon_1\sin\frac{\theta_1}{2}-\\-P_{11}\sin\varepsilon_1\cos\frac{\theta_1}{2})-\\-\frac{2\alpha_2}{\sqrt{\gamma_2}}(P_{22}\cos\varepsilon_2\sin\frac{\theta_2}{2}-\\-P_{21}\sin\varepsilon_2\cos\frac{\theta_2}{2})\end{array}\right.$$

where:

$$D=4\alpha_1\alpha_2-(1+\alpha_2^2)^2$$

$$P_{11}=(1+\alpha_2^2)\cosh\varepsilon(\pi-\theta_1)-2\eta\alpha_2\sinh\varepsilon(\pi-\theta_1)$$

$$P_{12}=(1+\alpha_2^2)\sinh\varepsilon(\pi-\theta_1)-2\eta\alpha_2\cosh\varepsilon(\pi-\theta_1)$$

$$P_{21}=\eta(1+\alpha_2^2)\sinh\varepsilon(\pi-\theta_2)-2\alpha_1\cosh\varepsilon(\pi-\theta_2)$$

$$P_{22}=\eta(1+\alpha_2^2)\cosh\varepsilon(\pi-\theta_2)-2\alpha_1\sinh\varepsilon(\pi-\theta_2)$$

$$\gamma_1=\sqrt{1-\frac{\rho v^2\sin^2\theta}{C_{11}}},\quad \gamma_2=\sqrt{1-\frac{\rho v^2\sin^2\theta}{C_{66}}}$$

$$\varepsilon_1=\varepsilon\ln\gamma_1,\quad \varepsilon_2=\varepsilon\ln\gamma_2$$

$$\tan\theta_1=\alpha_1\tan\theta,\quad \tan\theta_2=\alpha_2\tan\theta$$

ACKNOWLEDGMENT

This research was partially supported by the Ministry of Education and Science of Republic of Serbia through Grants ON174001 "Dynamics of hybrid systems with complex structures. Mechanics of materials", ON174004 "Micromechanics criteria of damage and fracture", TR 32036 "Development of software for solving the coupled multi-physical problems" and III41017 "Virtual human osteoarticular system and its application in preclinical and clinical practice".

REFERENCES

[1] Tippur H.V. and Rosakis A.J.: Quasi-static and dynamic crack growth along bimaterial interfaces: A note on crack-tip field measurements using coherent gradient tensor, Int. J. Fracture, Vol. 48, pp. 243-251, 1991.

[2] Rosakis A.J., Lee Y.J., Lambros J.: Dynamic Crack Growth in Bimaterial Interfaces, Experiments in Micromechanics of Failure Resistant Materials, AMD - Vol. 130, ASME, pp. 17-23, 1991.

[3] Yang, W., Suo Z., Shih C.F.: Mechanics of dynamic debonding, Proc. Roy. Soc. A, Vol. 433, pp. 679-697, 1991.

[4] Deng, X.: Complete complex series expansions of near-tip fields for steadily growing interface cracks in dissimilar isotropic materials, Eng. Fract. Mech., Vol. 42, No. 2, pp. 237-242, 1992.

[5] Lo, C.Y., Nakamura T.N. and Kushner, A.: Computational Analysis of Dynamic Crack Propagation along Bimaterial Interface, Int. J. Solid Struct., Vol. 31, pp. 145-168, 1992.

[6] Liu C., Lambros J. and Rosakis A.J.: Highly transient elastodynamic crack growth in bimaterial interface: higher order asymptotic analysis and optical experiments, J. Mech. Phys. Solids, Vol. 41, No. 12, pp. 1887-1954, 1993.

[7] Nikolic R.R. and Djokovic, J.M.: An approach to analysis of dynamic crack growth at bimaterial interface, Theor. and Appl. Mech., Vol. 36, No. 4, pp. 299-328, 2009.

[8] Willis, J.R.: The stress field near the tip of an accelerating crack, J. Mech. Phys. Solids, Vol. 40, No. 7, pp. 1671-1681, 1992.

[9] Nikolic R.R., Djokovic, J.M.: Mićunović, M.V.: The Competition Between the Crack Kinking Away From the Interface and Crack Propagation Along the Interface in Elastic Bicrystals, Int. J. Fracture, Vol. 164, No. 1, pp. 73-82, 2009.

[10] Rice J.R.: Elastic fracture mechanics concepts for interfacial cracks, J. Appl. Mech., Vol. 55, pp. 98 – 103, 1988.

[11] Hutchinson, J.W. and Suo, Z.: Mixed mode cracking in layered materials, J. Appl. Mech., Vol. 29. pp. 63 – 191, 1992.

[12] Wang T.C., Shih, C.F. and Suo, Z.: Crack extension and kinking in laminates and bicrystals, Int. J. Solid Struct., Vol. 29, pp. 327-344, 1992.

[13] Nikolic, R.R. and Djokovic, J.M.: Dynamic growth of Interfacial Cracks, in: Kubair , D. (Ed.) *Crack Growth: Rates, Prediction and Prevention*, Nova Publishers, Inc., New York, pp. 207-228, 2011.

[14] Djokovic, J.M. and Nikolic, R.R.: Characteristic Parameters of Dynamic Crack Growth Along the Interface Between the two Orthotropic Materials, Adv. Mater. Res., Vols. 452-453, Part 2, pp. 1184-1189, 2012.

[15] Freund, L.B.: *Dynamic Fracture Mechanics*, Cambridge University Press, Cambridge, 1990.

NOMENCLATURE

C_{ijkl}	the stiffness tensor
c_R	the Rayleigh's wave speed
v	the velocity
u_k	the displacements
p_i	the roots of the eq. (5)
$\boldsymbol{B}$	the Hermitian matrix defined in eq. (9)
$\boldsymbol{H}$	the bimaterial Hermitian matrix defined in eq. (9)
$\boldsymbol{A}$, $\boldsymbol{L}$	matrices defined in eq. (10)
R	Rayleigh's wave function, eq. (12)
$\boldsymbol{w}$	the unit vector
K	the complex stress intensity factor
K_3	the stress intensity factor for Mode III
r, θ	polar coordinates
$\boldsymbol{t}$	the interfacial force
G	the energy release rate
K^d,K_3^d	dynamic stress intensity factors

Greek symbols (Times New Roman 10 pt, bold, italic)

δ_{ij}	Kronecker delta
$\rho^{(i)}$	the material density
λ_i	introduced variables
α_i	the wave reduction factors defined in eq. (7)
ε	the oscillation index, eq. (15)
β	the Dundurs parameter, eq. (16)
σ_{ij}	stresses
$\tilde{\sigma}_{ij}^{1,2,3}(\theta)$	the angular functions which correspond to tensile tractions, in-plane shear tractions and anti-plane shear tractions across the interface
$\boldsymbol{\delta}(r)$	the crack opening displacement vector
$\boldsymbol{\lambda}$, ρ	nondimensional elastic parameters which measure anisotropy
η	the traction resolution factor, eq. (26)
τ	the energy factor, eq. (28)

Superscripts (Times New Roman 10 pt, bold, italic)

(1),(2)	values for material 1 and 2
d	dynamic

ДИНАМИЧКИ РАСТ ПРСЛИНЕ НА ИНТЕРФЕЈСУ ИЗМЕДЈУ ДВА АНИЗОТРОПНА МАТЕРИЈАЛА

Јелена М. Ђоковић, Ружица Р. Николић, Јожеф Вичан, Далибор Ђенадић

У раду је разматрано понашање напонског поља које окружује врх прслине која се динамички шири дуж интерфејса између два анизотропна материјала. Акценат је стављен на примену и проширење постојећег концепта механике лома на интерфејсу на проблем прслине која пропагира великом брзином. Приказана је угловна расподела напона за прслину која пропагира динамички. Разматрано је понашање осцилаторног индекса, фактора резолуције силе и фактора енергије у зависности од брзине врха прслине и односа крутости материјала.

Вредност осцилаторног индекса расте са порастом брзине пропагирања прслине и тежи бесконачности када се брзина приближава Раулеигх-евој таласној брзини мекшег материјала. Фактор резолуције силе јако зависи од брзине врха прслине али зато врло слабо од односа крутости. За фактор енергије важи обрнуто. Одређен је динамички фактор интензитета напона за анизотропну биматеријалну комбинацију за неколико основних конфигурација. Резултати добијени у овом раду могу да послуже као водич микромеханичком моделирању материјала.